Determination of pressure gradient in mitral stenosis with Doppler echocardiography

JARLE HOLEN AND SVEIN SIMONSEN

From the Department of Radiology, Department of Medicine B, and Institute for Surgical Research, University Hospital, Rikshospitalet, Oslo, Norway

SUMMARY   The accuracy of a non-invasive ultrasound Doppler technique for the determination of the pressure gradient in mitral stenosis was evaluated in a study of 8 adult patients. Transseptal left atrial catheterisation and retrograde left ventricular catheterisation were performed. The same diastoles were used to compare the gradient constructed from the ultrasound data ($\triangle P_U$) with that constructed from the manometric data ($\triangle P_M$). In the 8 patients the difference between the mean diastolic values of $\triangle P_U$ and $\triangle P_M$ was $- 0.54 \pm 1.0$ (SD) mmHg. The corresponding figure for mid-diastole was 0.01 ± 0.9 (SD) mmHg. The results indicate that the ultrasound technique is sufficiently accurate for diagnostic purposes.

In an initial study of a non-invasive ultrasound Doppler technique for the determination of the pressure gradient in mitral stenosis (Holen *et al.*, 1976) it was found that ultrasound can consistently register the frequency shifts from the diastolic mitral jet, and that the pressure gradient determined with ultrasound ($\triangle P_U$) agrees reasonably well with the manometric gradient ($\triangle P_M$) obtained from the pulmonary capillary venous and left ventricular pressures. Subsequent ultrasound studies of more than 150 patients with mitral stenosis have reinforced this impression.

Received for publication 30 November 1977

The present investigation was undertaken to explore the accuracy of the technique more closely by comparing $\triangle P_U$ with the manometric gradient obtained from left atrial (transseptal) and left ventricular pressures.

Subjects and methods

Data were collected from 8 adult patients undergoing routine preoperative cardiac catheterisation for mitral valve disease (Table).

ULTRASOUND SYSTEM
The frequency shifts from the mitral jet were

Table   *Data and numerical results on cases (gradients rounded off to nearest mmHg)*

Case no.	Age	Sex	HR	R	Q̇	Valve lesion	Gradients (mmHg)			
							Mean diastolic		Mid-diastolic	
							$\triangle P_U$	$\triangle P_M$	$\triangle P_U$	$\triangle P_M$
1	66	F	90	AF	3·1	MS, MR	14	14	15	15
2	52	M	68	SR	4·2	MS, MR, AR	7	8	8	8
3	54	M	64	SR	4·4	MS	11	13	10	11
4	66	F	58	SR	8·0	MS	4	5	3	5
5	46	F	60	AF	—	MS	13	13	11	11
6	66	F	76	AF	3·4	MS	9	8	9	9
7	30	M	86	AF	7·7	MS	13	13	13	12
8	56	M	70	SR	8·0	MS	11	12	9	9
X̄	55		72		5·6		10·3	10·8	9·8	10·0
SD	11		12		2·3		3·5	3·3	3·7	3·0

HR, heart rate; R, rhythm; Q̇, cardiac output (l/min); $\triangle P_U$, gradient from ultrasound data; $\triangle P_M$, gradient from manometric data; MS, mitral stenosis; MR, mitral regurgitation; AR, aortic regurgitation; SR, sinus rhythm; AF, atrial fibrillation; X̄, mean value; and SD, standard deviation.

obtained with a modified (Holen et al., 1976) 2·1 MHz continuous waveform Hewlett-Packard 8026B Sound Monitor. The ultrasound data were recorded on magnetic tape and subsequently frequency-analysed on a Kay Sona-Graph 6061B Sound Spectrum Analyzer. The hard copy of the frequency analysis is a grey scaled presentation wherein the abscissa is time and the ordinate frequency shift (Fig. 1b-4b). The degree of blackening at any particular point in the frequency analysis is in theory related to the energy present in the reflected sound, but electronic noise can also produce blackening. In the present investigation frequency analysis of the obtained Doppler spectrum was performed so that the time course of the maximum diastolic frequency shift ($\triangle f_{max}$) could be identified. In the frequency analysis $\triangle f_{max}$ is a curve drawn to envelop the blackening caused by the diastolic blood velocities. In order to identify $\triangle f_{max}$ as accurately as possible it is important that there is ample contrast between blackening from blood velocities and blackening from electronic noise. This contrast is in part dependent upon instrumentation, instrument settings, and ultrasound probe position.

MANOMETRIC SYSTEM

Left atrial and left ventricular pressures were obtained via 8F catheters. The catheters were connected to EMT-34 transducers (Elema Schönander) and pressures recorded by a Mingograph system.

COLLECTION OF DATA

The ultrasound and manometric data were collected simultaneously with the patient resting in the supine position. Immediately before the collection of data the optimum probe position on the patient's left anterior or lateral chest wall was identified with the aid of the audio signal of the Doppler spectrum (the optimum probe position is defined as that in which the incident sound beam is in acoustic contact with the diastolic mitral jet with its axis as closely aligned with the direction of the vectors with maximum diastolic velocity as is possible). This was accomplished by identifying the probe position where the audio signal of the diastolic Doppler spectrum seemed to contain the largest amount of high frequency sound. With the probe in the optimum position the ultrasound and manometric data were recorded simultaneously, provision being made for the identification of individual cardiac cycles in both so that the results from individual diastoles could be compared.

CONSTRUCTION OF GRADIENTS FROM ULTRASOUND AND MANOMETRIC DATA

The construction of the diastolic time course of the gradient from the ultrasound data was based upon three assumptions:

(1) The registered time course of $\triangle f_{max}$ reflected the maximum blood velocities in the mitral orifice.

(2) The probe position during data collection was such that the axis of the incident sound beam coincided with the direction of the vectors with maximum velocity in the orifice, thus allowing $\cos \theta = 1$ in the Doppler equation (Kinsler and Frey, 1962),

$$V_{max} = \frac{c \cdot \triangle f_{max}}{2 \cdot f \cdot \cos \theta} \quad \text{Doppler equation} \quad 1$$

Where, V_{max} = maximum blood velocity, c = velocity of sound in blood, $\triangle f_{max}$ = maximum frequency shift, f = frequency of incident sound beam, and θ = angle between axis of incident sound beam and direction of vectors with maximum blood velocity.

(3) The steady state orifice equation (eq. 2) (Streeter, 1961) is valid for the flow in stenotic mitral orifices

$$\triangle P = \tfrac{1}{2} \rho (V_{max})^2 \quad \text{Orifice equation} \quad 2$$

where $\triangle P$ = pressure gradient, ρ = mass density of blood, and V_{max} = maximum blood velocity.

$$\text{Thus, } \triangle P = \tfrac{1}{2} \rho \left[\frac{c \cdot \triangle f_{max}}{2 \cdot f \cdot \cos \theta} \right]^2$$

$$\text{And } \triangle P = \tfrac{1}{2} \rho \left[\frac{c^2}{2^2 \cdot f^2 \cdot \cos^2\theta} \right] \cdot \triangle f_{max}^2$$

Using $c = 1.57 \cdot 10^5$ cm/s (Hertz, 1977), $f = 2.1 \cdot 10^6$ Hz, $\cos \theta = 1$, and $\rho = 1.06/981$ g s² per cm⁴ (Diem and Lentner, 1962) and using 1·36 for mmHg conversion yields the following working equation

$$\triangle P =$$

$$\frac{1}{1.36} \cdot \frac{1}{2} \cdot \frac{1.06}{981} \left[\frac{1.57^2 \cdot 10^{10}}{2^2 \cdot 2.1^2 \cdot 10^{12}} \right] \cdot \triangle f_{max}^2 \cdot 10^6$$

$$\text{or } \triangle P_U = 0.55 \cdot \triangle f_{max}^2 \quad 3$$

where $\triangle P_U$ = pressure gradient determined from ultrasound data (mmHg) and $\triangle f_{max}$ = maximum diastolic frequency shift (kHz).

The time course of $\triangle f_{max}$ was drawn by hand on the hard copy of the frequency analysis as a curve enveloping the blackened areas representing diastolic blood velocities. The time course of $\triangle P_U$ was then constructed from $\triangle f_{max}$ using eq. 3. The time course of the manometric gradient ($\triangle P_M$) was constructed from the values obtained by subtracting the left ventricular diastolic pressure from the left atrial diastolic pressure.
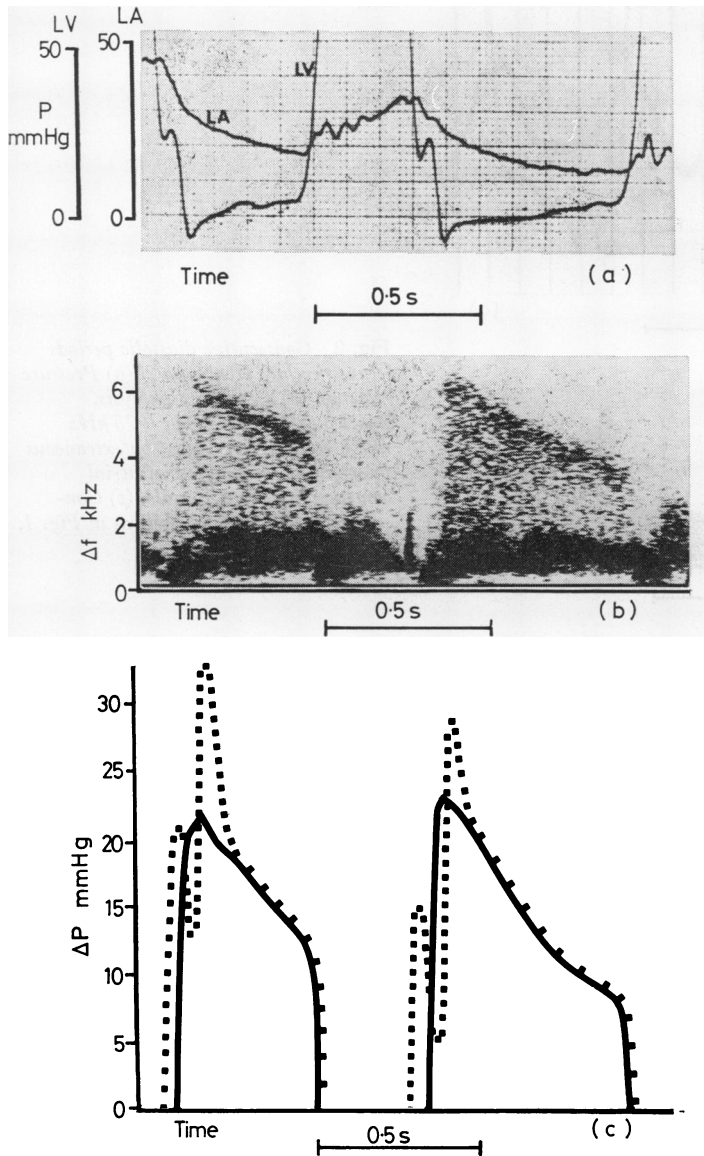
Fig. 1 *Two consecutive diastolic periods (atrial fibrillation) from case 1. (a) Pressure tracings. P, pressure; LV, left ventricle; LA, left atrium. (b) Frequency analysis. △f, frequency shift. A hypothetical curve enveloping blackened diastolic areas will represent time course of maximum diastolic frequency shift. Note blackened band of about 0·5 kHz width adjacent to maximum frequency shift (most prominent in the first diastolic period). (c) Constructed gradients. △P, pressure gradient; ———, gradient from ultra- sound data; - - -, gradient from manometric data.*

COMPARISON OF △P$_U$ AND △P$_M$

In general gradients were constructed from 3 to 4 consecutive diastolic periods in each patient. Comparisons were made of the mean diastolic and the mid-diastolic values of △P$_U$ and △P$_M$.

Results

Representative pressure recordings, frequency analyses, and constructed gradients are presented in Fig. 1 to 4. In any given patient there was minimal variation in the quality of the recordings. A total of 28 diastolic periods were analysed and the gradients constructed.

The curve representing △f$_{max}$ was drawn by hand as a line demarcating the relatively heavy blackening caused by blood velocities from the lighter blackening produced by electronic noise. With the exception of the extremes of diastole the accuracy with which the location of △f$_{max}$ could be determined was estimated as ± 1/8 (SD) kHz. According to eq. 3 this corresponds to ± 0·4 (SD),
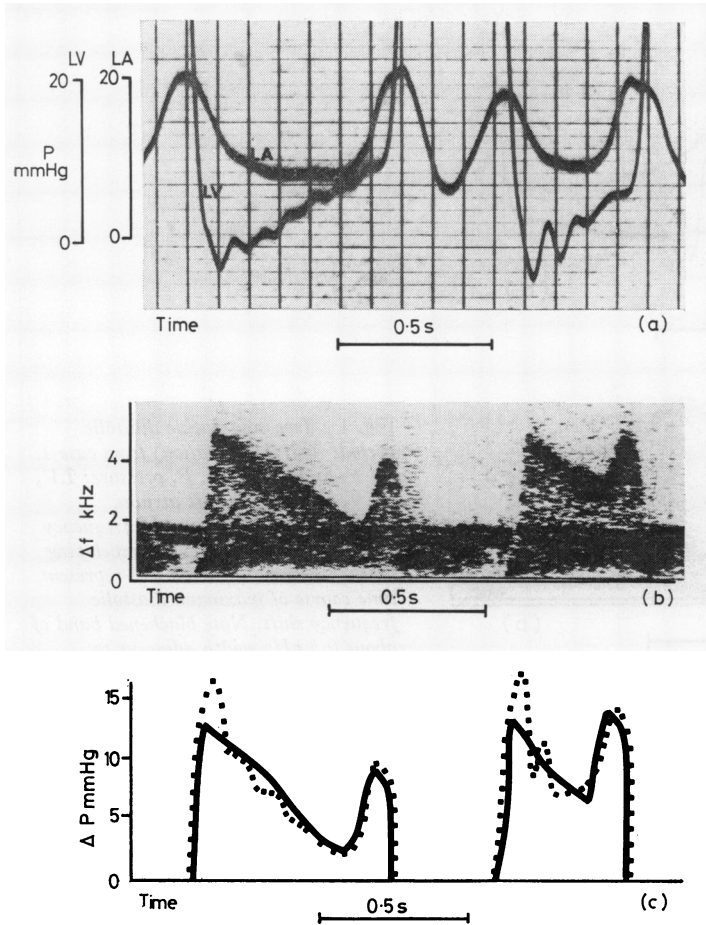
Fig. 2 *Consecutive diastolic periods (sinus rhythm) from case 2. (a) Pressure tracings. (b) Frequency analysis. Blackened band of about 0·75 kHz width at 2 kHz is caused by extraneous interference. Note effect of atrial contraction in late diastole. (c) Constructed gradients. Symbols as in Fig. 1.*

$\pm$ 0·6 (SD), $\pm$ 0·7 (SD), and $\pm$ 0·8 (SD) mmHg for gradients of 5, 10, 15, and 20 mmHg, respectively. Near the extremes of diastole where Δf_{max} was less than 2 kHz the frequency shifts caused by the mitral jet were obscured in some patients by blackening from valve motion and ventricular blood velocities. In these regions Δf_{max} was drawn as a straight line continuation of the definable part of the curve.

The rate of change with time of Δf_{max} was greatest immediately after the onset of diastolic flow and immediately before its cessation. Relatively rapid changes in Δf_{max} also occurred during atrial contraction, whereas in general conditions approaching a steady state prevailed in mid-diastole (Fig. 1b to 4b).

With the exception of one patient (Fig. 4b), the frequency analyses exhibited a band of relatively heavy blackening adjacent to Δf_{max} in the mid-portion of diastole.

The left ventricular pressure tracings showed early diastolic oscillation in all patients (Fig. 1a to 4a) and the effect of this oscillation was prominent in the constructed time course of ΔP_M (Fig. 1c to 4c). Similar oscillation was not observed in the frequency analyses or in left atrial pressure tracings. In patients in sinus rhythm the effect of atrial contraction was distinctly shown in both ΔP_U and ΔP_M (Fig. 2c to 4c). In early diastole and during atrial contraction, peak ΔP_M invariably exceeded peak ΔP_U. The major discrepancies between ΔP_U and ΔP_M were found in association with these gradient peaks.

In the 8 patients the mean diastolic value of ΔP_M was 5 to 14 mmHg (Table). The difference between the mean diastolic value of ΔP_U and the mean diastolic value of ΔP_M was $-$ 0·54 $\pm$ 1·0 (SD) mmHg. The corresponding value for the mid-diastolic gradients was 0·01 $\pm$ 0·9 (SD) mmHg.
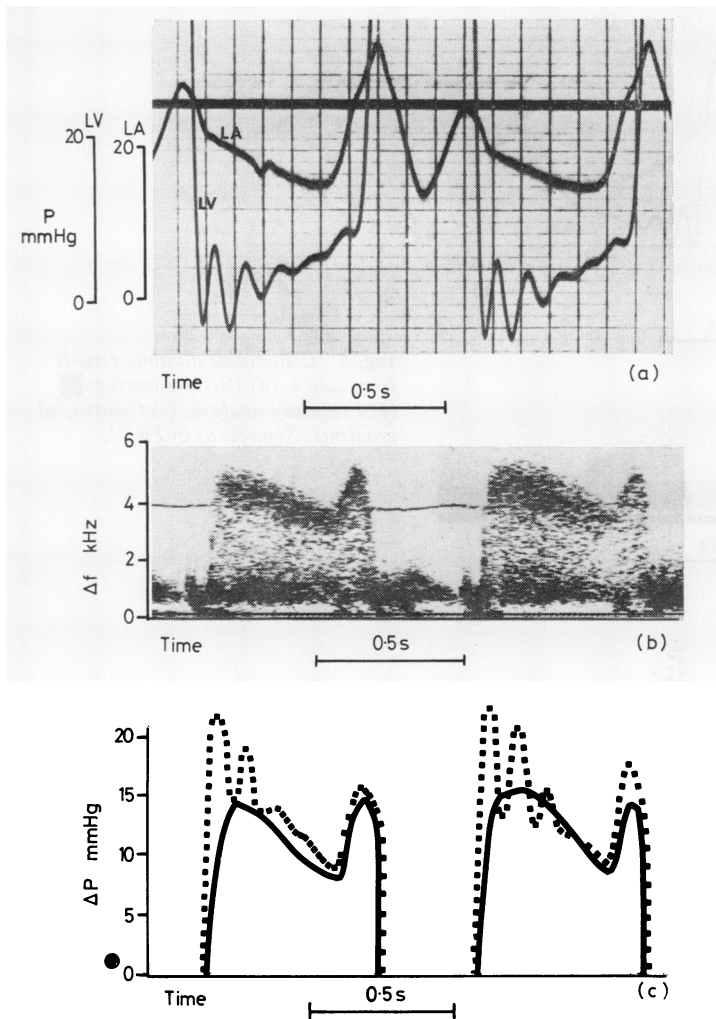
Fig. 3 *Consecutive diastolic periods from case 3. (a) Pressure tracings. Note oscillation in tracing from left ventricle. (b) Frequency analysis. (c) Constructed gradients. Symbols as in Fig. 1.*

Discussion

The liquid-filled catheters used in the manometric system are likely to produce significant errors in $\triangle P_M$ in the vicinity of the rapid pressure changes. The oscillation in the left ventricular pressure tracings supports this contention. Peak values and timing of $\triangle P_M$ therefore may well be erroneous.

The pressure gradient in mitral stenosis can be considered as the sum of an inertial and a dissipative (frictional loss) component. The steady state orifice equation (eq. 2) neglects the inertial component; thus $\triangle P_U$ will also misrepresent the actual gradient during rapid pressure changes and this can be

expected to influence the value of the mean diastolic gradient more than the mid-diastolic one. The finding that agreement between mid-diastolic values of $\triangle P_U$ and $\triangle P_M$ was slightly better than that between mean diastolic values may reflect this; alternatively, it is possible that the difference in agreement is chiefly the result of errors in $\triangle P_M$. In any event it appears that neglect of the inertial component of the gradient has only a minimal influence on the agreement between the mean diastolic values of $\triangle P_U$ and $\triangle P_M$.

The orifice equation also neglects frictional losses incurred upstream of the flow sector where blood velocity is at its maximum. The mid-diastolic agree-
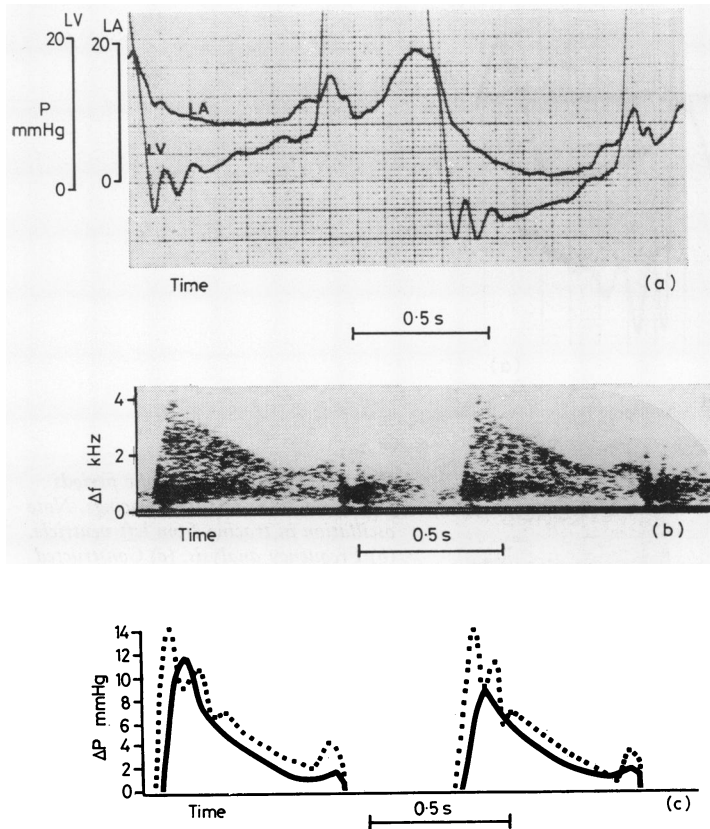
Fig. 4 *Consecutive diastolic periods from case 4. (a) Pressure tracings.* ■ *(b) Frequency analysis. (c) Constructed gradients. Symbols as in Fig. 1.*

ment found between $\triangle P_U$ and $\triangle P_M$ indicates, however, that the equation predicts the dissipative component of the pressure gradient with reasonable accuracy. This conclusion is supported by the results of previously described *in vitro* studies of the equation (Holen *et al.*, 1977).

Failure to achieve a probe position where the axis of the incident sound beam coincides with the direction of the vectors with maximum velocity can theoretically lead to a major underestimation of the actual pressure gradient (eq. 1). The confidence that can be placed in the ultrasound technique is undoubtedly enhanced if satisfactory probe positioning can be confirmed by inspection of the frequency analyses, for previous experience with the technique has indicated that the blackened band adjacent to $\triangle f_{max}$ in the mid-portion of diastole is a sign of this. The band is believed to be the result of the incident sound beam traversing the left ventricle along the mitral jet and thus exposes a large volume of high velocity blood. Failure to achieve correct probe positioning may thus account for the

relatively large mid-diastolic discrepancy between $\triangle P_U$ and $\triangle P_M$ found in case 4. Clearly, the effects of probe position on the appearance of the frequency analyses warrant further study.

Conclusions

(1) This ultrasound technique appears to determine mean and mid-diastolic mitral valve gradients with an accuracy that is sufficient for diagnostic purposes. (2) The accuracy of the technique is chiefly limited by the accuracy with which $\triangle f_{max}$ can be determined from the frequency analyses. (3) The orifice equation (eq. 2) predicts the dissipative component of the pressure gradient with an accuracy that is acceptable for diagnostic purposes. (4) Neglect of the inertial component of the pressure gradient influences the value of the mean gradient very little. (5) A satisfactory probe position ($\cos \theta = 1$ in eq. 1) can be attained in the majority of patients with mitral stenosis and can probably be confirmed by inspection of the frequency analyses.

References

Diem, K., and Lentner, C. (1962). *Documenta Geigy Scientific Tables*, 6th edn, p. 547. J. R. Geigy, Basle.

Hertz, H. (1977). Principles of ultrasound in medical diagnosis. In *Echocardiography with Doppler Applications and Real Time Imaging*, p. 11. Martinus Nijhoff Medical Division, The Hague.

Holen, J., Aaslid, R., Landmark, K., and Simonsen, S. (1976). Determination of pressure gradient in mitral stenosis with a non-invasive ultrasound Doppler technique. *Acta Medica Scandinavica*, **199**, 455-460.

Holen, J., Aaslid, R., Landmark, K., Simonsen, S., and Østrem, T. (1977). Determination of effective orifice area in mitral stenosis from non-invasive ultrasound Doppler data and mitral flow rate. *Acta Medica Scandinavica*, **201**, 83-88.

Kinsler, L. E., and Frey, A. R. (1962). *Fundamentals of Acoustics*, 2nd edn, p. 489. Wiley, New York.

Streeter, V. L. (1961). *Handbook of Fluid Dynamics*, pp. 3-21. McGraw-Hill, New York.